ORIGINAL ARTICLE





Establishment of a Biaxial Testing System for Characterization of Right Ventricle Viscoelasticity Under Physiological Loadings

Kellan Roth¹ · Wenqiang Liu^{2,3} · Kristen LeBar¹ · Matt Ahern^{1,2} · Zhijie Wang^{1,2}

Received: 10 March 2022 / Accepted: 19 February 2024 © The Author(s) under exclusive licence to Biomedical Engineering Society 2024

Abstract

Purpose Prior studies have indicated an impact of cardiac muscle viscoelasticity on systolic and diastolic functions. However, the studies of ventricular free wall viscoelasticity, particularly for that of right ventricles (RV), are limited. Moreover, investigations on ventricular passive viscoelasticity have been restricted to large animals and there is a lack of data on rodent species. To fill this knowledge gap, this study aims to develop a biaxial tester that induces high-speed physiological deformations to characterize the passive viscoelasticity of rat RVs.

Methods The biaxial testing system was fabricated so that planar deformation of rat ventricle tissues at physiological strain rates was possible. The testing system was validated using isotropic polydimethylsiloxane (PDMS) sheets. Next, viscoelastic measurements were performed in healthy rat RV free walls by equibiaxial cyclic sinusoidal loadings and stress relaxation. **Results** The biaxial tester's consistency, accuracy, and stability was confirmed from the PDMS samples measurements. Moreover, significant viscoelastic alterations of the RV were found between sub-physiological (0.1 Hz) and physiological frequencies (1–8 Hz). From hysteresis loop analysis, we found as the frequency increased, the elasticity and viscosity were increased in both directions. Interestingly, the ratio of storage energy to dissipated energy (W_d/W_s) remained constant at 0.1–5 Hz. We did not observe marked differences in healthy RV viscoelasticity between longitudinal and circumferential directions.

Conclusion This work provides a new experimental tool to quantify the passive, biaxial viscoelasticity of ventricle free walls in both small and large animals. The dynamic mechanical tests showed frequency-dependent elastic and viscous behaviors of healthy rat RVs. But the ratio of dissipated energy to stored energy was maintained between frequencies. These findings offer novel baseline information on the passive viscoelasticity of healthy RVs in adult rats.

Keywords Hysteresis · Storage energy · Dissipated energy · Relaxation modulus · Silicone

Associate Editor Sarah Vigmostad, Ph.D. oversaw the review of this article.

☑ Zhijie WangZhijie.Wang@colostate.edu

Published online: 11 March 2024

- Department of Mechanical Engineering, Colorado State University, Fort Collins, CO, USA
- School of Biomedical Engineering, Colorado State University, Fort Collins, CO, USA
- Stanford Cardiovascular Institute, Stanford University, Stanford, CA, USA

Introduction

Heart failure (HF) results from structural or functional impairment of ventricular filling or ejection of blood [1]. Data from 2012 to 2016 shows an estimated 6.2 million Americans above 20 years old have HF [2]. The importance of both left and right ventricle (LV and RV) function has been recognized in HF [3–5]. It is known that the mechanical behavior of ventricular tissues contributes to the diastolic function and the tissue biomechanics change during HF development. Moreover, prior research of myocardial viscoelasticity using cardiomyocytes (CM) or papillary muscles has shown an influence of cellular viscoelasticity on myocardial contractile function [5–8]. However, investigations of ventricular free wall viscoelasticity are few and restricted to large animals, and there is no report on rodent



ventricular viscoelasticity using the common mechanical testing methods.

Historically, there has been a lack of experimental evidence that ventricular free wall exhibits significant hysteresis during cyclic deformation [9], and the field of cardiac tissue biomechanics has focused on the hyperelastic behavior of the complex microstructure of the tissue. Recently, more evidence of viscoelasticity is reported for both the LV and RV with a marked viscoelastic behavior. These studies include ex vivo tissue mechanical tests on adult porcine LV [10], adult human LV and RV [11], neonatal porcine LV and RV [12], as well as adult ovine LV and RV from our group [13]. Nevertheless, there is little viscoelastic measurement in rodent ventricles using the well-established ex vivo mechanical testing techniques (i.e., uniaxial, biaxial or triaxial tensile/compression tests or shear tests) [3]. Because rodents are the most frequently used species for preclinical cardiac research [4, 14], the knowledge of ventricular tissue viscoelasticity from rodents needs to be established.

Viscoelasticity is time-dependent, meaning that the mechanical behavior depends on the rate at which a material is deformed. Since the heart deforms nonlinearly and at varying heart rates for different species, the characterization of ventricular viscoelasticity in non-linear motion and at cardiac cycle-like stretch rates of the species is required to invoke physiologically relevant information. We reviewed the current biaxial testers reported in the literature of ventricular mechanical studies, with the specifics of these commercial or in-house built testers listed in Table 1. Among these ex vivo studies, the heart samples (LV and/or RV) were typically biaxially stretched at a stretch rate of 0.1 to 0.75 mm/s [12, 15–17] for loading/unloading stress-strain curve measurement or at set frequencies of 0.01-0.5 Hz [11, 18, 19] for cyclic mechanical tests. All these tests were performed at sub-physiological deformation rates even for large animal species (heart rate ~ 1 Hz). In some studies in heart valves, higher stretch rates have been applied to the sample using a commercial biaxial testing system (Electro-Force®) [20, 21]. However, only the elastic behavior was investigated from the 'J'-shaped stress-strain curve, and it remains unclear if the synchronous acquisition of the force and image data is ensured.

To obtain the viscoelastic property of rodent heart tissues in physiological states, it would require a much faster deformation of the sample. That is, assuming the average heart rate of 250–500 bpm for rats [22, 23] and the physiological strain at end-diastole of 15–20%, the biaxial tensile tester should generate ~5–8 Hz of cyclic stretch or a strain rate of ~100-160% per second. Assuming a sample size of 10×10 mm², this would require a stretch rate of ≥ 100 mm/s and sufficient data sampling rates of ≥ 80 Hz. Additionally, the force sensor should have a relevantly small working range considering the small loads exerted by the rodent tissue

[24–27]. After a close examination of all existing biaxial testers in Table 1 and the availability of the commercial parts used in these systems, none of them can achieve the required specifications as stated above. Moreover, most of the custom systems conducted linear deformation in cyclic loadings and the nonlinear physiological conditions were not replicated. Therefore, a new biaxial tester is needed to induce nonlinear (sinusoidal) cyclic deformation at the heart rates of rodents to capture the tissue's viscoelastic behavior under physiological loadings.

The aim of this research is to establish a biaxial testing system for rat RV viscoelasticity measurement via non-linear cyclic deformation of ventricle samples across physiological heart rates. Such a testing system will offer valuable information of the ventricular viscoelasticity for rodents, which are commonly used species in preclinical models of cardiac research. Relevant to the present study, this tester will enable the characterization of RV passive viscoelasticity under physiological conditions (e.g., resting or acute stress) and provide novel knowledge of the anisotropic, viscoelastic behavior of healthy rat RVs.

Materials and Methods

Biaxial Tester Design and Construction

A block diagram of the components involved in the biaxial testing system is shown in Fig. 1. To reach the desired physiological deformations, we firstly determined the required specifications for the actuators, load cells, and camera of the testing system. The maximal required velocity of the actuators is 62.8 mm/s (assuming a sample size of 10×10 mm² at the maximum stretch of 25% and cycle frequency of 8 Hz for rat heart tissues). For load cells, because the reported peak stress of rodent RVs does not exceed 50 kPa [24-27]in both healthy and diseased states, a sensor with the maximal force within 25 N would be sufficient. For image acquisition, it is reasonable to achieve 20–40 frames per cycle (i.e., 160–320 fps) with an image resolution of 1000 pixels \times 1000 pixels. Based on these prerequisites, the following equipment were therefore selected: two actuators (model XDMQ-DE, Zaber, Vancouver, British Columbia) with the maximal velocity of 1400 mm/s, a camera (model BLXT-17 M, Baumer, Frauenfeld, Switzerland) with the maximal sampling rate of 660 fps and the maximal resolution of 1100×1600 pixels, and two 5-lb (22.5 N) load cells (model 31, Honeywell, Charlotte, North Carolina). Finally, a desktop PC (HP Z4 Workstation, Palo Alto, California) was selected based on the processing and memory requirements from the camera, as well as the connections compatible with all electrical components. All equipment was compatible with LabVIEW as the agent for movement control and data acquisition.



Table 1 Summary of key components in existing custom or commercial biaxial systems used for ventricular or valve leaflet mechanical studies, as well as some relevant systems for non-cardiac research

System	Actuators	Force sensors	Image acquisition	Reported stretch rate	Reported testing type	Reference(s)
Custom	L9221 (by Airpax Inc.)	1000 g (by Sensotec Honeywell)	LC1901KAN-011 Camera (2048×2048 pixels, EG&G)	22.86 mm/s,	Cyclic	[25]
Custom	NA	10N	NA	7.5 mm/s	Cyclic	[16]
Custom	NA	100N	NA (Laser extensometer)	30 mm/s	Cyclic	[11, 19, 26, 27]
Custom	NA (by Harvard apparatus)	F5-A (by Konigsberg)	Model 4410 Video Camera (Cohu Instru- ments)	2.5 mm/s	Cyclic	[28]
Custom	NA	NA	Model WV- 3260/8AF Video Camera (1000 FPS, Panasonic)	NA	Cyclic	[29]
Custom	404XR (by Parker Han- nafin)	Model 31 (250 g, Sensotec Honeywell)	Fast Camera 13 (1240×1024 pixels, 1000 FPS, Fast Vision LLC)	1000 mm/s	Cyclic	[12, 17, 23, 30]
Custom	T-LLS105 (by Zaber Technologies)	Model 31 (250 g, Sensotec Honey- well)	Grasshopper3 Camera (4.2 MP, 18 FPS, Point Grey)	6 mm/s	Cyclic, stress relaxation	[31, 32]
Custom	DS4 series (by Kollmorgen)	LSB210 (44.48N, Futek)	Mako G-419B Camera (2048×2048 pixels, 26 FPS, Allied Vision)	500 mm/s	Cyclic	[33]
Custom	MicroTester Actuators (by Instron)	5N or 500N	NA	15.7 mm/s	Cyclic	[34]
CellScale Biotester (Cellscale.com)	NA	0.5–23N options available	1280×960 pixels, 15 FPS	20 mm/s	Cyclic	[15, 18, 21, 22]
TestResources 574LE2 (TestRe- sources.net)	NA	100N	NA	Capable of 15 Hz	Cyclic	[35]
TA Instruments ElectroForce® planar biaxial TestBench	NA	NA	NA, 30–240 FPS	NA (0.001–1 Hz)	Cyclic	[20]
TA Instruments ElectroForce® planar biaxial TestBench	NA	NA	NA, 30–455 FPS	NA (2.5–12.4 Hz)	Cyclic	[21]

NA indicates unavailable or unspecified information

Nonindustrial components of the tester were designed based on the size, orientation, and fastening connection specifications compatible with the actuators and load cells. To minimize the shear deformation during the planar biaxial mechanical tests, linear guides (SSEB series, MiSUMi Corporation, Schaumburg, Illinois) were set perpendicular to the arms to allow free lateral movement. Parts were manufactured using computer numeric control milling, hand lathe

and milling, and 3D printing processes. All geometry configurations (size, thickness) of the sample were obtained by caliper measurements. To track the local strain/deformation of the sample, four markers were placed equidistant from the center of the specimen in a square geometry, and a digital image correlation algorithm was applied to the images, as described previously [27–29]. A photo of the tester with all hardware assembled is shown in Fig. 2.



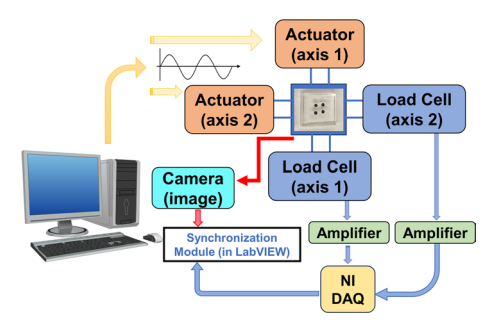


Fig. 1 Block diagram of biaxial tester components. A square sample is mounted to four arms of the system via tines to allow the motion and recording of the force in two perpendicular directions (longitudinal and circumferential). Two arms are connected to the actuators, which receive a simultaneous command to induce cyclic sinusoidal deformation in the samples. The other two arms are connected to the load cells and amplifiers which acquire simultaneous biaxial forces in the sample. An in-house LabVIEW module is used to synchronize the force and image signals.

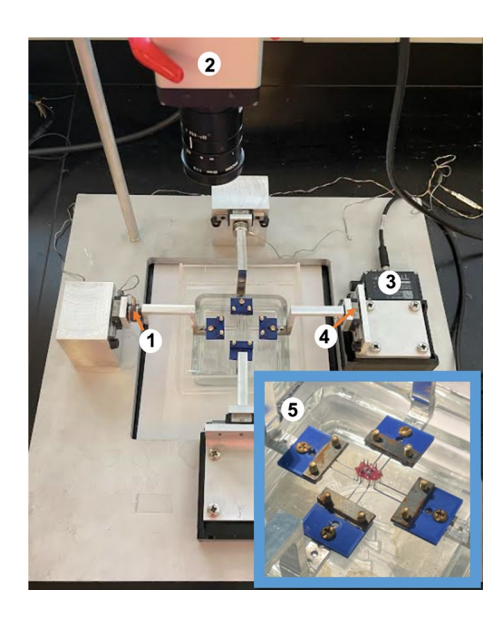
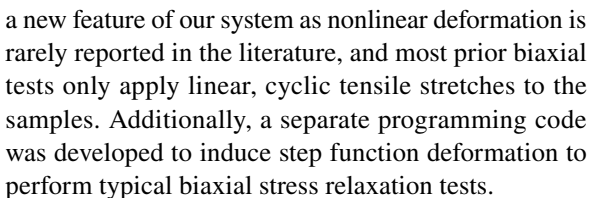


Fig. 2 Snapshot of the biaxial tester with key components labeled. Load cell (1), camera (2), actuator (3), movement rail (4), and a close-up picture of the system mounted with a rat RV sample (5)

Software Development

The in-house LabVIEW codes were developed for performing biaxial cyclic sinusoidal tensile tests and stress relaxation at various stretch rates. The MATLAB codes were adapted from prior studies [13, 28, 30] for additional viscoelastic property quantification. The functional modules include:

(a) Synchronized sinusoidal (nonlinear) stretch and stress relaxation in two axes: The ASCII programming code was developed to achieve synchronized sinusoidal (nonlinear) movement of the biaxial actuators. This is



- (b) Synchronized image and force data acquisition: We developed a customized LabVIEW interface ('module') for the control of the image acquisition and storage at 200 fps. Because of the constraints in the image resolution and exposure time, the maximal sampling rate achieved was 200 fps to obtain sufficient resolution in the image frame. The image acquisition was achieved through the "grab" camera function and a producer-consumer loop setup in LabVIEW. To induce synchronized recording of force and image data, an image timestamp function was used to record the time of image acquisition by the camera (rather than the time of image frame received by LabVIEW) while the load cell data was sampled simultaneously and relayed via two in-line amplifiers into a USB DAQ (NI USB-6002, National Instruments) with the same internal time clock.
- (c) Strain analysis: Finally, a customized MATLAB code was developed for 2D strain analysis, using four equally spaced markers in the center region as fiducials to track the deformation of the sample as described previously [24, 26, 27, 31].

System Validation

Polydimethylsiloxane (PDMS) Sheet Testing

To evaluate the tester capability, an isotropic, synthetic material was used. We chose polydimethylsiloxane (PDMS, commonly referred to as silicone) as the material due to its frequent use in the biomedical field including cardiovascular applications [32]. A PDMS sheet (Sylgard 184, Dow Corning, Midland, MI) was prepared using a 10:1 base to curing agent mass ratio. The mixture was cured in a stainless-steel container in a vacuum oven maintained at room temperature for 48 hours to remove all gas bubbles from the material. For mechanical tests, samples were cut into $15\times15\times3$ mm³ sheets (N = 3), mounted and preloaded to 0.1 N in room air. After 10 preconditioning cycles [33], the sample was stretched equibiaxially under either cyclic sinusoidal deformation or stress relaxation. These tests served for validation purposes of the following capabilities:

(a) Capability to induce biaxial, cyclic sinusoidal stretches at various frequencies:



To evaluate if the actuator can move at various stretch rates nonlinearly, equibiaxial tensile testing of PDMS samples was conducted. Samples were deformed in sinusoidal motion at 20% of maximal strain, at 0.1, 1, 2, 5 and 8 Hz. The inclusion of these frequencies was to test the capability of the system to measure a material's viscoelastic behavior at a broad range of frequencies from sub-physiological to physiological stretch rates. We used 0.1 Hz testing frequency as a sub-physiological testing condition, although the system can operate under much lower stretch rates (e.g., 0.001 Hz). The 1 Hz and 2 Hz testing frequencies correspond to the resting and exercising heart rates of a human or large animal species, and the 5 Hz and 8 Hz frequencies correspond to the resting and exercising heart rates of a rat. Thus, these are all physiologically relevant stretch rates from small to large animal species. Moreover, our new system could function under nonlinear (sinusoidal) deformation cycles, which is rarely reported in soft tissue mechanical tests. The force curves were then acquired to confirm the successful induction of biaxial motions at these frequencies.

(b) Capability to induce biaxial stress relaxation at various ramp speeds and strains:

To evaluate if the ramp speed can reach the diastolic stretch rate of a rat heart, samples were deformed by a brief linear stretch (ramp) followed by a constant deformation at desired strain levels. This could simulate the tissue deformation from diastolic filling (ramp) to the following isovolumic contraction (maintained stretch) phases [34]. Stretch rate was determined by Eqn.1, assuming that the heart tissue is deformed at 20% of strain at end diastole, and there are approximately equal periods of diastole and systole per cardiac cycle (T). Moreover, at the fixed ramp speed mimicking the resting heart rate (HR) of rats (300 bpm), stress relaxation was performed at different strain magnitudes (3%, 6%, 9%, 12%, 15%) to examine the type of viscoelastic behavior of PDMS sheets as described previously [35, 36].

$$Stretch \, rate = \frac{\Delta L}{T/2} \tag{1}$$

where cardiac cycle T = 1/HR (seconds), and $\Delta L = 0.2 \times unloadedlength(L_0)$ (mm).

(c) Consistency of measurements between two axes:

We next compared the experimental curves of isotropic PDMS samples under equibiaxial loading to confirm the consistency of the measurements from two axes (longitudinal and circumferential). Using the data obtained from cyclic sinusoidal loading, the stress-strain hysteresis loops from different axes were compared for each frequency.

(d) Accuracy and stability of the system:

To evaluate the accuracy of the biaxial tester, PDMS samples (N=3) were subjected to equibiaxial cyclic loading under the same conditions as described above. Force and image data were obtained, and the stress-strain hysteresis curves were derived. The average and standard error of the elastic (elastic modulus) and viscous (Tan (δ) , where δ is the phase shift between stress and strain data) properties of the PDMS were calculated (see §2.4 for details) and compared to similar parameters found in literature reports [37–40].

Rat RV Testing

Finally, we measured the biaxial viscoelastic properties of RV tissues from healthy adult rats. The novel viscoelastic measurement of rodent RVs demonstrated the successful acquisition of ventricular viscoelasticity in physiological states for small animal species for the first time. All procedures were approved by Colorado State University IACUC (protocol #1438). Prior to tissue harvest, 8-10-week-old male Sprague Dawley rats (Envigo, US) (N = 12) were euthanized by urethane (1.2-1.5 g/kg, i.p. injection) or carbon dioxide. Prior to the mechanical tests, the RV tissue was excised, measured, and then placed in cardioplegic solution (CPS) combined with 30 mM of 2,3-butanedione monoxime (BDM) heated solution at 37 °C for 30 minutes to ensure full relaxation of cardiomyocytes. The outflow tract (OT) direction was used as the longitudinal axis, while the perpendicular direction was the circumferential axis. Each sample was glued with 4 equally spaced markers for strain analysis.

After mounting, the samples were preloaded and underwent 15 cycles of equibiaxial stretch at 1 Hz and 20% of strain for preconditioning. Then similarly as done for PDMS samples, cyclic sinusoidal equibiaxial tensile tests with 20% of strain at 0.1, 1, 2, 5, and 8 Hz were performed (N=9) with sufficient resting periods between tests equivalent to 10 times the testing period. In stress relaxation tests, samples were linearly stretched at different ramp speeds (corresponding to 0.1, 1, 2, 5 and 8 Hz of cycle tests) and then held at a constant strain of 20% (N=12). The entire mechanical testing was performed at a temperature of 26–37 °C.

Viscoelastic Data Analysis

From the cyclic sinusoidal tensile tests, an average hysteresis stress-strain loop can be derived from the last three cycles. For synthetic samples (see §2.3.1), engineering stress P and engineering strain ε were derived for each direction $(P = F/A_0, \varepsilon = dl/l_0)$, where F is the measured force, l_0 is the initial length, and A_0 is the initial cross-section area. For biological samples (see §2.3.2), the 2^{nd} Piola-Kirchhoff (PK) stress (S) and Green strain (E) were derived for each



direction ($\sigma = \lambda P$, $S = P/\lambda$, and $E = (\lambda^2 - 1)/2$), where σ is Cauchy stress and λ is the stretch, as previously described [29].

Next, the overall elastic modulus (M) was derived as the slope of the linear fitting of the entire hysteresis loop, and the viscosity was represented by the phase shift (δ) between the stress and strain data (Fig. 3 and Eqn.2). Furthermore, the stored energy (W_S) and dissipated energy (W_d) were calculated from the hysteresis loop as shown in Fig. 3 as indices of elasticity and viscosity, respectively. These methods are adapted from previous studies [13, 30].

$$\delta = \operatorname{asin}\left(\frac{W}{B}\right) \tag{2}$$

where W=hysteresis loop width at $\frac{1}{2}$ maximal stress; B = maximal strain.

To examine the type of viscoelastic behavior of PDMS from stress relaxation, different relaxation rates were calculated as the slopes of linear fitting to logarithmic stress vs. time plots at different strain magnitudes (3–15%). Nonlinear viscoelasticity is confirmed if the relaxation curves from the different strain magnitudes are not parallel, which is measured through statistical significance. To examine the viscoelastic relaxation of rat RVs, biaxial stress relaxation was performed at various stretch rates corresponding to 0.1–8 Hz and at the strain of 15%. The relaxation modulus and normalized stress obtained at 0.01 seconds after the peak stress were used to represent the relaxation behavior of the tissue. These methodologies are described previously [13, 41].

Statistical Analysis

All data are shown as mean \pm SE. Statistical significance was determined as p < 0.05 with a student's t-test.

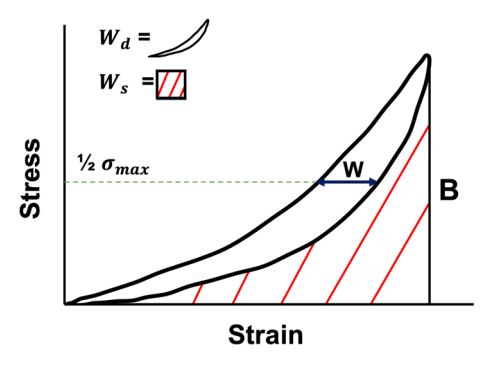


Fig. 3 Stress strain hysteresis loop showing stored (W_s) and dissipated (W_d) energy as well as the maximal strain (B) and the loop width at half of the maximal stress (W). Stored energy is calculated as the area beneath the unloading curve, and dissipated energy is calculated as the area within the hysteresis (loading and unloading curves)

Results

System Validation by PDMS Sheets

Firstly, we examined if the biaxial tester was capable of achieving planar biaxial tensile tests at the desired deformations. The silicone sheet was successfully deformed by cyclic loadings at various frequencies (from 0.1 to 8 Hz). The sinusoidal force generated from the cyclic stretch of the actuators confirmed the non-linear (sinusoidal) deformation of the samples (Fig. 4a). We observed similar sinusoidal force data curves from the longitudinal direction at the same testing frequencies. We further examined the relaxation response of PDMS sheets under equibiaxial stress relaxation. The tester successfully induced the linear stretch of the sample in the ramping phase at the desired stretch rates corresponding with various heart rates (0.1–8 Hz) (Fig. 4b). We observed that the peak force tended to increase with an increasing stretch rate.

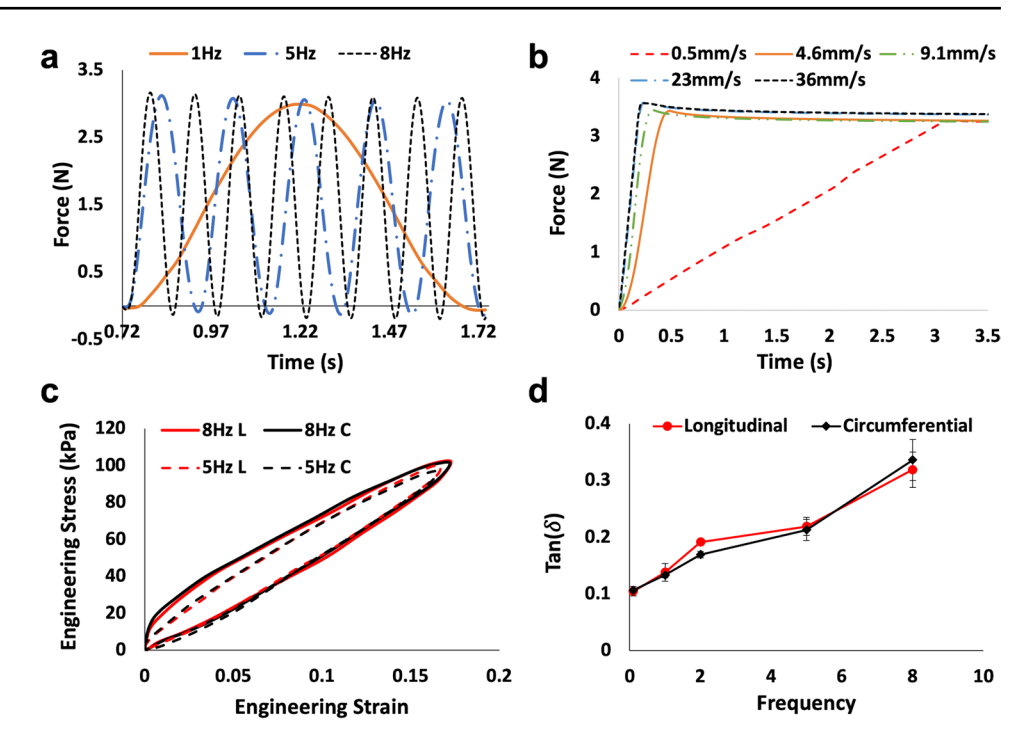
Moreover, we examined if consistent, synchronized viscoelasticity measurements were achieved between the two axes of the system. This character is especially important for high-speed cyclic tests to mimic the physiological deformations of rodent hearts. Under biaxial cyclic loadings, the stress-strain hysteresis loops of PDMS sheets obtained from two axes (at both 5 and 8 Hz) were identical (Fig. 4c). The loading and unloading curves at each individual frequency well overlapped, confirming the tester's ability to accurately capture the PDMS's isotropic mechanical behavior. Moreover, we examined the shear deformation which was negligible compared to the planar deformation (data not shown).

We further derived the viscoelasticity parameters of PDMS sheet by using the elastic moduli (M) and $\tan(\delta)$, both of which are commonly reported in literature. The average M measured across all frequencies was 0.54 ± 0.01 MPa in the longitudinal direction and 0.58 ± 0.01 MPa in the circumferential direction, respectively. As expected, we observed frequency-dependent increase in these viscoelastic parameters of PDMS sheets. The average M ranged from 0.51 ± 0.004 to 0.60 ± 0.02 MPa as frequency increased. The viscosity (phase shift) also increased with increasing frequency, ranging from 0.11 ± 0.005 to 0.33 ± 0.03 across the testing frequencies (Fig.4d). Moreover, the overlapping of the $\tan(\delta)$ curves in the longitudinal and circumferential directions for this isotropic material again confirmed the consistent measurements between the two axes.

Finally, in the viscoelastic measurements of PDMS sheets, the standard error (SE) was within $\pm 8\%$ of the mean for the testing frequency up to 5 Hz. We observed a slightly larger SE at the testing frequency of 8 Hz, but the percentage of deviation is acceptable ($\pm 10.3\%$ of the mean).



Fig. 4 Validation of the biaxial tester with PDMS sheets. a Representative force-time data from cyclic biaxial tests recorded at varying frequencies in the circumferential direction. b Representative circumferential force-time data from stress relaxation recorded at varying stretch rates (mm/s) that correspond to heart rates of 0.1-8 Hz. c Representative longitudinal and circumferential stress-strain hysteresis loops at physiological frequencies of rats that indicate consistent viscoelastic measurements in different axes. d Frequency-dependent viscosity of PDMS sheets measured by $tan(\delta)$ in circumferential and longitudinal directions



PDMS Exhibits Nonlinear Viscoelastic Behavior Within 15% Strain

From this study, we also investigated the type of viscoelastic behavior of the silicone (PDMS) material. By performing stress relaxation at different strain magnitudes, we examined if the relaxation behavior depended on strain levels as previously reported [35, 36]. The strain-dependent relaxation behavior shows that the silicone material is nonlinear viscoelastic. As shown in Fig. 5, we observed identical stress relaxation behavior at most of the strains (6-15%). However, the fitting of the 3% strain curve was significantly different than the fitting slopes of other strain curves in both directions (except for the 6% longitudinal data). Thus, the data showed that the relaxation behavior of PDMS sheets was

strain-dependent, and the PDMS exhibited nonlinear viscoelastic behavior.

Healthy Rat RV Biaxial Viscoelasticity Characterization

Frequency-Dependent Viscoelastic Behavior from Cyclic Loadings

Next, we obtained the biaxial viscoelastic behavior of healthy rat RV samples under cyclic sinusoidal loadings at 0.1–8 Hz. Our data showed strain-rate (or frequency) dependent changes in the hysteresis loops (Fig. 6). In both directions, as the frequency increased, the slope of the loop increased, and the area of the loop got larger. This indicates

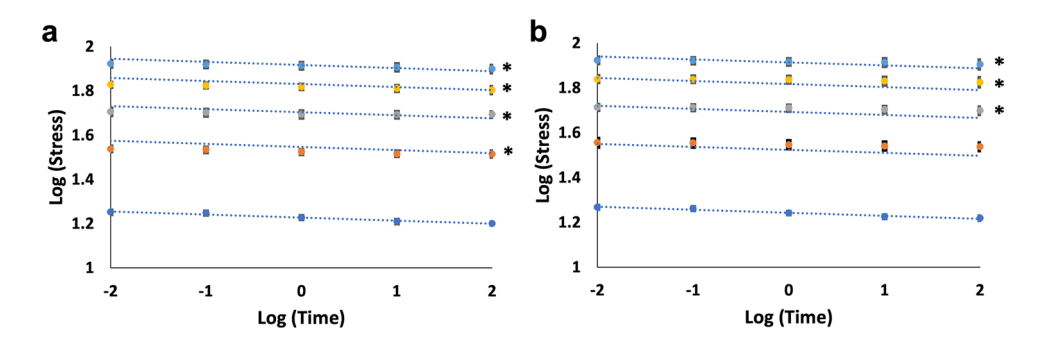
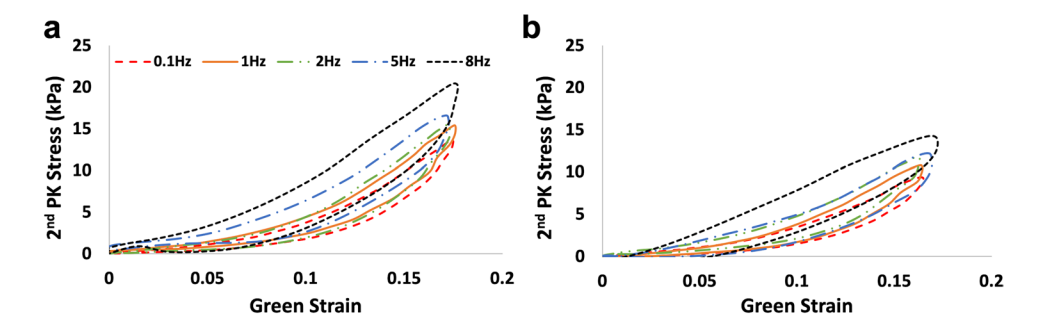


Fig. 5 Log scale plots of stress relaxation of PDMS sheets. Viscoelastic characterization of PDMS sheets in longitudinal (a) and circumferential (b) directions were obtained from stress relaxation at the

ramp speed corresponding with a heart rate of 5 Hz. Blue dashed line: the fitted line at 3% strain superimposed onto the other strain levels. *p<0.05 vs slope of 3%



Fig. 6 Frequency-dependent stress-strain hysteresis loops of rat RVs obtained from equibiaxial cyclic loadings. Representative stress-strain loops in the longitudinal (a) and circumferential (b) directions are shown



an increased elasticity and viscosity of the RV tissue at a higher deformation rate.

We further quantified the stored (W_s) and dissipated (W_d) energy as well as the M of the RV samples from the hysteresis loops. We found that these parameters were increased with increasing testing frequency in both directions (Fig. 7). Significant increases in stored and dissipated energy were observed from the sub-physiological (0.1 Hz) to physiological (1-8 Hz) stretch rates. Additionally, in the longitudinal direction (Fig. 7a), the increase in W_d was more pronounced at 8 Hz and the increase in W_s was more markedly at 5 Hz. In the circumferential direction (Fig. 7b), the W_s was increased more significantly at 5 and 8 Hz, while the W_d was increased more significantly at 8 Hz. Examining the M showed that, although frequency-dependent increase was observed in both directions, the increase was more pronounced in the circumferential direction (Fig.7c). These data suggest that the viscoelastic behavior between the sub physiological (0.1–2 Hz) and physiological (5–8 Hz) deformations were distinct, which support the necessity to measure rat RV viscoelasticity under physiological conditions (in nonlinear and fast deformations). Moreover, there was no significant difference of these viscoelastic parameters between the longitudinal and circumferential directions at all testing frequencies. This suggests an isotropic viscoelastic behavior of the health rat RV samples.

Lastly, we examined the change in the ratio of stored to dissipated energy (W_d/W_s) as a function of frequency. As shown in Fig. 7d, the ratio W_d/W_s was maintained at a constant level across most testing frequencies (up to 5 Hz) in both directions. The only exception was the ratio at 8 Hz where a significant increase was observed compared to all other frequencies.

Frequency-Dependent Relaxation Behavior from Stress Relaxation

Next, we examined the frequency-dependent relaxation behavior of the rat RV from the stress relaxation data. We observed a significant frequency-dependent decrease in relaxation modulus in both the longitudinal and circumferential directions (Fig. 8a). Similarly, the frequency-dependent

Fig. 7 a. b The stored (W_a) and dissipated (W_d) energy of rat RVs obtained from the longitudinal and circumferential direction, respectively. c The elastic modulus (M) derived from the entire loop in both directions. d The ratio of stored and dissipated energy (W_d/W_s) in both directions. *p < 0.05 vs. 0.1 Hz from the same direction. $\dagger p < 0.05$ vs. 1 Hz from the same direction. p < 0.05 vs 2 Hz from the same direction. &p < 0.05 vs 5 Hz from the same direction

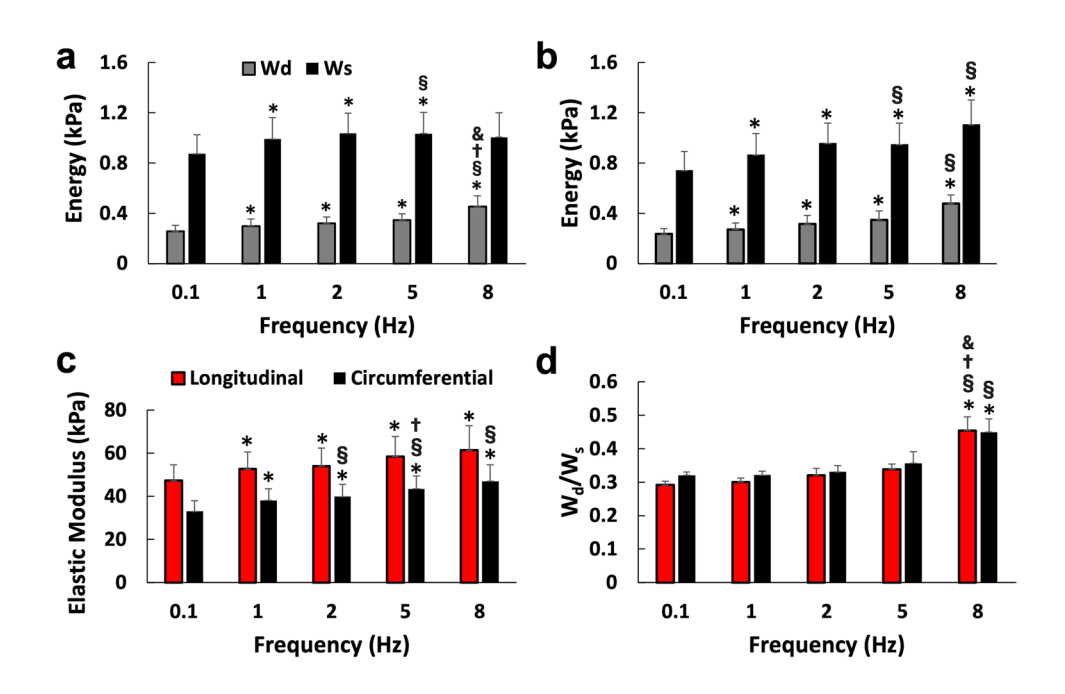
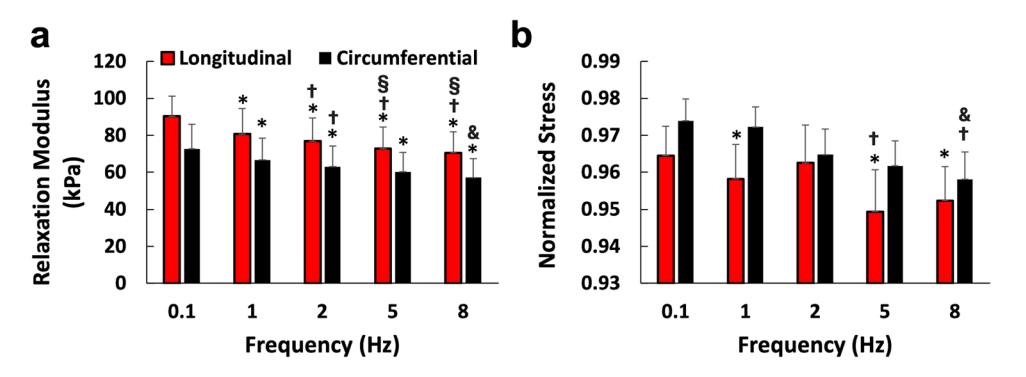




Fig. 8 Relaxation behavior of rat RVs obtained at various ramp speeds corresponding to frequencies of 0.1–8 Hz. a relaxation modulus and **b** normalized stress were quantified at 0.01 s after the peak stress. *p < 0.05 vs. 0.1 Hz from the same direction. †p < 0.05 vs. 1 Hz from the same direction. \$p < 0.05 vs 2 Hz from the same direction. &p < 0.05 vs 5 Hz from the same direction.



decrease in normalized stress was observed in both directions, particularly at physiological frequencies of 5 and 8 Hz (Fig. 8b). The decreases of relaxation modulus and normalized stress with increasing frequency indicate that the rat RV is relaxing faster at higher stretch rates.

Discussion

The objective of this study was to develop a biaxial testing system for rat RV viscoelasticity characterization under physiological loadings. In the present work, we have constructed and validated the testing system by synthetic, isotropic PDMS sheets. Further, we characterized the viscoelastic behavior of PDMS at 0-15% of strain, confirming a nonlinear viscoelastic behavior of the material. We further characterized the rat RV free wall viscoelasticity by equibiaxial cyclic loadings and stress relaxation using physiological strain rates. We found that the rat RV exhibited increased viscoelastic behavior from quasi-static to physiological stretch rates under cyclic tensile tests, which suggests the importance of characterizing the tissue viscoelastic properties under in vivo loading conditions. An interesting 'homeostasis' condition of the constant ratio of stored to dissipated energy (W_d/W_s) was observed across frequencies of 0.1–5 Hz. Overall, the RV exhibited isotropic viscoelastic behavior in healthy, adult rats. To our knowledge, this is the first characterization of healthy rat RV passive biaxial hysteresis in physiological states. The novel set of data will advance the knowledge of RV biomechanics in both energy storage and energy dissipation functions.

System Validation with PDMS Sheets

Firstly, from the force curves we confirmed that the new tester could deform samples at the desired stretch rates corresponding to the frequency of 0.1–8 Hz and in sinusoidal (nonlinear) motions. As the stretch rate increased (e.g., at 5 and 8 Hz), we observed some minor 'over-shoot' (~6%) of the peaks and valleys as shown in Fig. 4a The actuators have a built-in servo motor positioning loop, and

the position of the actuators is consistently monitored and corrected. The observed overshoot may be attributed to the non-adjustable, built-in controller tuning. Additionally, inertia from the mass of the components at high deformation rates could contribute to the overshoot. Then, we evaluated the tester's capability to perform stress relaxation with a ramping speed mimicking the physiological diastolic filling of the heart at resting or exercised heart rate. The tester was able to stretch samples equibiaxial at these commanded stretch rates. From the quasi-static (0.5 mm/s) to physiological stretch rates (23–36 mm/s), the peak force was increased and the normalized stress was reduced, indicating the increased instantaneous elasticity and enhanced relaxation behavior of the PDMS sheets (Fig. 4b).

Thirdly, we confirmed that the viscoelastic behaviors of PDMS measured across both axes were consistent. The stress-strain loops under cyclic loadings were similar between the axes across all testing frequencies, although only those at the physiological frequencies (5 and 8 Hz) were shown (Fig. 4c). Furthermore, a viscous indicator measured by $\tan(\delta)$ (phase shift) showed consistent values between the longitudinal and circumferential axes for most frequencies including the 5 and 8 Hz. Therefore, using an isotropic material, we assessed and confirmed the equal performance of the two axes in measuring viscoelastic properties.

Next, we examined the frequency-dependent viscoelastic behavior of the PDMS using commonly reported parameters derived from the hysteresis. Overall, we found an increase in elasticity as the frequency (stretch-rate) increased. The average elastic moduli across all frequencies were 0.54~0.58 MPa. These values are within the reported range in the literature (0.5 MPa to 1.8 MPa at various frequencies and strains, with different loading conditions) [32, 39, 42]. The variation of the tensile elastic modulus of PDMS may be induced by several factors such as humidity or water content in the polymers [43], curing temperature [42], and the base to curing agent ratio of Sylgard 184 [32]. Since not all these details were provided from prior studies, we did not require an exact match of the value with that in literature. Our measured values fell within the range seen by previous studies.



From the viscosity measurements via $tan\delta$ (Fig. 4d) and the hysteresis loop area (data not shown), we found that both parameters were increased with increasing testing frequency. Such frequency-dependent viscous behavior is consistent with the previous reports [39, 42]. The study by Goyal et al. is the only one, to our knowledge, that reports frequency-dependent viscoelasticity in the same frequency range (1–8 Hz) and same condition (in room air) as ours. But the $\tan\delta$ values found in our study are approximately 2× larger than the former study, however they follow the same increasing trend [39]. A few reasons may explain the discrepancy. The former test was non-constrained uniaxial test and performed at 30% of strain. Also, insufficient details were provided in the PDMS fabrication process and other aspects of the mechanical testing protocol, which may affect the PDMS sheets viscoelasticity and measurement values. Overall, the PDMS mechanical data demonstrated that the new testing system enabled biaxial viscoelastic measurement of soft materials under the required physiological loadings for rodents.

Characterization of PDMS Viscoelasticity Type at 0–15% Strain

PDMS is used in many biomedical contexts including the cardiovascular applications [32]. However, to our knowledge, a full characterization of PDMS (silicone) viscoelasticity has not been documented. A viscoelastic material can be linear viscoelastic, quasi-linear viscoelastic (QLV), or fully nonlinear viscoelastic (NLV). The nonlinear viscous behavior is revealed by a strain-dependent relaxation behavior. Most biological tissues including the myocardium exhibit a fully nonlinear viscoelastic behavior [13, 41, 44], but whether the PDMS is NLV is unclear. In terms of the elastic behavior, a previous study found that PDMS was linearly elastic only between 0 and 40% of tensile strain [40], although this measurement was conducted at a quasi-static rate of 0.33 mm/s. From the cyclic tests at 0-20% strain in this study, we observed linear elastic behavior from the elliptical shape of the hysteresis. To examine if the viscous behavior of PDMS is linear or not, we compared the stress relaxation curves at different strains (3–15%) using a fixed ramping speed (22.8 mm/s). Because the fitted line to the curve at 3% strain was not in parallel with the fitted lines to the curves at higher strains (6–15%) (Fig. 5), the viscous behavior was strain-dependent (nonlinear). Our data indicates that PDMS is a nonlinear viscoelastic material at 0-15% strain in room temperature condition.

This behavior is not completely surprising as some polymers have been shown to display a nonlinear viscoelastic behavior [45]. The nonlinear viscoelastic behavior of solid polymers is dependent on conditions such as temperature and loading conditions [46]. Previously the

PDMS was found to exhibit nonlinear elastic behavior at strains > 40% [40]. Our study, to our knowledge, is the first to report a nonlinear viscoelastic behavior of PDMS when deformed at cardiac physiological loading conditions. The characterization of the viscoelastic behavior of PDMS at the strain and stretch rate similar to those observed in the physiological deformation of myocardium will assist to develop more biomimetic materials for various biomedical or tissue engineering applications using silicone polymers.

Characterization of Stretch-Rate Dependent Biaxial Viscoelasticity of Rat RVs

Using the new biaxial tester, we proceeded to conduct the original biaxial viscoelastic measurements of the rat RV free wall. The RV showed significant increases in viscosity and elasticity with increasing stretch rate in both directions (Figs. 6 and 7). By examining the stored (W_s) and dissipated (W_d) energy as well as the elastic moduli (M) of the RV samples, we observed significant increases in both elasticity and viscosity not only from quasi-static to dynamic stretch rates (> = 1 Hz), but also between physiological stretch rates (5 and 8 Hz). The stretch-rate dependent mechanical behavior was similarly found in heart valves, and the stress-strain relations obtained under physiological stretch rates are different than those obtained under quasi-static or sub-physiological stretch rates [20, 21]. We then concluded that to approach the physiological viscoelasticity measurement of rat RVs, a testing protocol that induces physiological loadings is imperative.

Using stress relaxation, we additionally saw significant decreases in relaxation modulus and normalized stress with the increasing ramp speed, further indicating the importance of using physiological stretch rates to inform the tissue's viscoelasticity. Moreover, these results showed that at faster deformations the relaxation rate became faster, indicating an enhanced viscous damping of the material. Another phenomenon we noticed was the different effects of stretch rate on peak stress and relaxation modulus in PDMS material. As seen in the PDMS material, increased peak stress (Fig. 4b) and reduced relaxation modulus (data not shown) were observed as the stretchrate increased. But in the RV tissue, reduced peak stress (data not shown) and relaxation modulus (Fig. 8a) were observed as stretch-rate increased. We are not entirely clear about the molecular mechanism that determines these relaxation parameters, but we speculate the complex composition of RV tissue (including myofibers, collagen fibers, and other viscoelastic components) may result in a different recruitment of 'biological polymers' than the synthetic, single-type polymers in PDMS. Therefore, the trends of these parameters may not be consistent.



Isotropic Viscoelastic Behavior and Potential 'Homeostasis' in W_d/W_s of Rat RVs

From both cyclic loading and stress relaxation data, we did not observe statistically significant differences between the longitudinal and circumferential directions. This suggests an isotropic viscoelastic behavior of healthy rat RVs. However, the longitudinal direction showed a trend of larger elastic modulus (Fig. 7c) as well as a trend of larger relaxation modulus (Fig. 8a) than the circumferential direction. Prior studies on the elastic behavior of rat or ovine RVs found that the elasticity was significantly higher in the longitudinal than circumferential direction [3, 24, 25]. A histology examination showed that the fiber orientation was altered transmurally, spreading from the longitudinal (outflow tract) direction by about a 90 degree-dispersion to the circumferential direction [24]. We suspect that the wide dispersion of the myo- and collagen fiber orientation transmurally and the new dynamic loading conditions here could affect the recruitment of these biological constituents and lead to the isotropic viscoelastic behavior observed in this study.

Another new finding from the rat RV is about the 'preservation' of the ratio W_d/W_s. Interestingly, despite larger variations in elasticity (W_c) or viscosity (W_d) (Fig. 7a and b), the variation in the ratio of W_d/W_s (Fig. 7c) was relatively small and it remained constant across most frequencies (0.1–5 Hz). This suggests a mechanical or thermal 'homeostasis' condition of the tissue that is independent of the strain rate (and of individual subjects). Traditionally, the elastic and viscous properties are separately discussed as they represent different mechanical behaviors. However, a recent study has suggested a potential prognostic value of the ratio of viscous to elastic behavior. The cardiomyocytes from HFrEF patients presented lower W_d/W_s than those from HFpEF patients [5]. The baseline data from the healthy rat RVs here seem to bring additional evidence in support of homeostasis for the optimal viscoelastic function of the RV tissue. The physiological implications of the maintenance or change of the ratio in response to varied loadings awaits further investigation.

Limitations

There are several areas for improvement in the biaxial tester. We saw a higher variance in the cyclic tests at 8 Hz than other lower frequencies. This may be related to the overshoot of the cyclic stretches, or the current approach adopted in LabVIEW to synchronize the force and image data acquisition. We therefore did not over-interpret the data obtained at this testing frequency. Additionally, each mounting arm only had two mounting rakes for the easy operation on the small sized samples. Increasing rake number will induce a more homogeneous stress field [47]. For the mechanical

testing of the rat RV, the samples were not sustained at 37 °C throughout testing. A temperature-controlled tissue bath should be implemented in the future. Finally, there are a couple of factors neglected in mechanical tests. The lowest frequency in the cyclic tests was 0.1 Hz, which was considered sub-physiological but not quasi-static. Thus, the 'elastic baseline' information of the tissue was not obtained. Moreover, we did not obtain failure strain or natural recoil rate of the samples in our experiments. Both provide useful information for tissue mechanics. Future mechanical testing protocol should take these factors into consideration.

Conclusions

This research effort has culminated in a new biaxial tester that is functioning for the measurement of passive, anisotropic viscoelastic properties of ventricular free wall in small animal species under physiological conditions. The viscoelastic properties of healthy rat RVs were characterized, and a frequency dependence of the viscoelasticity was found, where increased viscoelasticity was significant from quasi-static to physiological stretch rates. This suggests that characterizing heart tissue viscoelasticity in in vivo loading conditions is important. We additionally observed a 'homeostasis' condition of the ratio of stored to dissipated energy across 0.1–5 Hz of frequencies along with isotropic viscoelasticity in these specimens. The research provides a new experimental tool to quantify the passive, biaxial viscoelastic behavior of ventricles in both small and large animals, and the findings in healthy rat RVs offer critical baseline information about the viscoelasticity of healthy RV free wall.

Acknowledgements We would like to express our gratitude to Katie Evans and Michael Nguyen-Truong for assisting in data collection, and Ethan Barron for helping in tissue bath construction.

Declarations

Conflict of interest Kellan Roth, Wenqiang Liu, Kristen LeBar, Matt Ahern and Zhijie Wang declare that they have no conflict of interest.

References

- Yancy, C. ACCF/AHA guideline for the management of heart failure: executive summary: a report of the American College of Cardiology Foundation/American Heart Association task force on practice guidelines. J. Am. Coll. Cardiol. 128(16):1810, 2013.
- Virani, S. S., and W. T. Connie. Heart disease and stroke statistics-2020 update: a report from the american heart association. Circulation. 141(9):139, 2020.
- Liu, W., and Z. Wang. Current understanding of the biomechanics of ventricular tissues in heart failure. *Bioengineering*. 7:2, 2020. https://doi.org/10.3390/BIOENGINEERING7010002.



- Kia, D. S., K. Kim, and M. A. Simon. Current understanding of the right ventricle structure and function in pulmonary arterial hypertension. *Front. Physiol.* 12:641310, 2021.
- Caporizzo, M. A., C. Y. Chen, K. Bedi, K. B. Margulies, and B. L. Prosser. Microtubules increase diastolic stiffness in failing human cardiomyocytes and myocardium. *Circulation*. 2020. https://doi. org/10.1161/CIRCULATIONAHA.119.043930.
- Caporizzo, M. A., C. Y. Chen, A. K. Salomon, K. B. Margulies, and B. L. Prosser. Microtubules provide a viscoelastic resistance to myocyte motion. *Biophys. J.* 115(9):1796–1807, 2018. https:// doi.org/10.1016/j.bpj.2018.09.019.
- Cooper, G. Proliferation cardiac microtubules. Heart Circul. Physiol. 297:H510, 2009.
- 8. Cooper, G. Cytoskeletal networks and the regulation of cardiac contractility: microtubules, hypertrophy, and cardiac dysfunction. *Heart Circul. Physiol.* 291(3):1003–1014, 2006.
- 9. Gultekin, O., G. Sommer, and G. A. Holzapfel. An orthotropic viscoelastic model for the passive myocardium: continuum basis and numerical treatment. *Comput. Methods Biomech. Biomed. Eng.* 19(15):1647–1664, 2016.
- Dokos, S., B. H. Smaill, A. A. Young, and I. J. LeGrice. Shear properties of passive ventricular myocardium. *Heart Circul. Physiol*. 283(6):2650–2659, 2002.
- Gerhard, S., et al. Biomechanical properties and microstructure of human ventricular myocardium. *Acta Biomater*. 24:172–192, 2015. https://doi.org/10.1016/J.ACTBIO.2015.06.031.
- Ahmad, F., et al. Biomechanical properties and microstructure of neonatal porcine ventricles. *J. Mech. Behav. Biomed. Mater.* 88:18–28, 2018.
- Liu, W., M. Nguyen-Truong, M. Ahern, K. M. Labus, C. M. Puttlitz, and Z. Wang. Different passive viscoelastic properties between the left and right ventricles in healthy adult ovine. *J. Biomech. Eng.* 2021. https://doi.org/10.1115/1.4052004.
- 14. Borgdorff, M. A. J., M. G. Dickinson, R. M. F. Berger, and B. Bartelds. Right ventricular failure due to chronic pressure load: What have we learned in animal models since the NIH working group statement? *Heart Fail. Rev.* 20:475–491, 2015.
- Fatemifar, F., M. D. Feldman, M. Oglesby, and H. C. Han. Comparison of biomechanical properties and microstructure of trabeculae carneae, papillary muscles, and myocardium in human heart. J. Biomech. Eng. 2018. https://doi.org/10.1115/1.4041966.
- Sirry, M. S., et al. Characterisation of the mechanical properties of infarcted myocardium in the rat under biaxial tension and uniaxial compression. J. Mech. Behav. Biomed. Mater. 63:252–264, 2016.
- Ghaemi, H., K. Behdinan, and A. D. Spence. In vitro technique in estimation of passive mechanical properties of bovine heart: Part I. Experimental techniques and data. *Med. Eng. Phys.* 31(1):76– 82, 2009.
- Javani, S., M. Gordon, and A. N. Azadani. Biomechanical properties and microstructure of heart chambers: a paired comparison study in an ovine model. *Ann. Biomed. Eng.* 44(11):3266–3283, 2016. https://doi.org/10.1007/S10439-016-1658-7.
- Nordsletten, D., et al. A viscoelastic model for human myocardium. Acta Biomater. 135:441–457, 2021.
- Anssari-Benam, A., Y.-T. Tseng, G. A. Holzapfel, and A. Bucchi. Rate-dependency of the mechanical behaviour of semilunar heart valves under biaxial deformation. *Acta Biomaterilia*. 88:120–130, 2019.
- Anssari-Benam, A., Y.-T. Tseng, G. A. Holzapfel, and A. Bucchi. Rate-dependent mechanical behaviour of semilunar valves under biaxial deformation: from quasi-static to physiological loading rates. *J. Mech. Behav. Biomed. Mater.* 104:103645, 2020.
- Milani-Nejad, N., and P. M. L. Janssen. Small and large animal models in cardiac contraction research: advantages and disadvantages. *Pharmacol. Ther.* 141(3):235–249, 2014.

- Sharp, J., T. Zammit, T. Azar, and D. Lawson. Stress-like responses to common procedures in individually and grouphoused female rats. *Contemp. Top. Lab Anim. Sci.* 42(1):9–18, 2003.
- Hill, M. R., M. A. Simon, D. Valdez-Jasso, W. Zhang, H. C. Champion, and M. S. Sacks. Structural and mechanical adaptations of right ventricle free wall myocardium to pressure overload.
 Ann. Biomed. Eng. 42(12):2451–2465, 2014. https://doi.org/10.1007/s10439-014-1096-3.
- Jang, S., et al. Biomechanical and hemodynamic measures of right ventricular diastolic function: translating tissue biomechanics to clinical relevance. *J. Am. Heart. Assoc.* 2017. https://doi.org/10. 1161/JAHA.117.006084.
- Valdez-Jasso, D., M. A. Simon, H. C. Champion, and M. S. Sacks. A murine experimental model for the mechanical behaviour of viable right-ventricular myocardium. *J. Physiol.* 590:4571, 2012.
- Avazmohammadi, R., M. Hill, M. Simon, and M. Sacks. Transmural remodeling of right ventricular myocardium in response to pulmonary arterial hypertension. *APL Bioeng.* 2017. https://doi.org/10.1063/1.5011639.
- Labus, K. M., and C. M. Puttlitz. An anisotropic hyperelastic constitutive model of brain white matter in biaxial tension and structural–mechanical relationships. *J. Mech. Behav. Biomed. Mater.* 62:195–208, 2016.
- Liu, W., et al. Multiscale contrasts between the right and left ventricle biomechanics in healthy adult sheep and translational implications. *Front. Bioeng. Biotechnol.* 10:588, 2022. https://doi. org/10.3389/FBIOE.2022.857638/BIBTEX.
- Wang, Z., R. S. Lakes, J. C. Eickhoff, and N. C. Chesler. Effects of collagen deposition on passive and active mechanical properties of large pulmonary arteries in hypoxic pulmonary hypertension. *Biomech. Model Mechanobiol.* 12:1115–1125, 2013.
- Gupta, K. B., M. B. Ratcliffe, M. A. Fallert, L. H. Edmunds Jr., and D. K. Bogen. Changes in passive mechanical stiffness of myocardial tissue with aneurysm formation. *Circulation*. 89(5):2314– 2326, 1994.
- Kim, J. H., P. Chhai, and K. Rhee. Development and characterization of viscoelastic polydimethylsiloxane phantoms for simulating arterial wall motion. *Med. Eng. Phys.* 91:12–18, 2021.
- Fung, Y. C., K. Fronek, and P. Patitucci. Pseudoelasticity of arteries and the choice of its mathematical expression. *Heart Circ. Physiol.* 237(5):620–631, 1979.
- Caporizzo, M. A., and B. L. Prosser. Need for speed: the importance of physiological strain rates in determining myocardial stiffness. *Front. Physiol.* 2021. https://doi.org/10.3389/FPHYS.2021.696694.
- Liu, W., et al. Alterations of biaxial viscoelastic properties of the right ventricle in pulmonary hypertension development in rest and acute stress conditions. *Front. Bioeng. Biotechnol.* 2023. https:// doi.org/10.3389/fbioe.2023.1182703.
- Liu, W., et al. Strain-dependent stress relaxation behavior of healthy right ventricular free wall. *Acta Biomater*. 152:290–299, 2022. https://doi.org/10.1016/J.ACTBIO.2022.08.043.
- Mata, A., A. J. Fleischman, and S. Roy. Characterization of polydimethylsiloxane (PDMS) properties for biomedical micro/nanosystems. *Biomed. Microdev.* 7:281–293, 2005.
- Sales, F. C. P., R. M. Ariati, V. T. Noronha, and J. E. Ribeiro. Mechanical characterization of PDMS with different mixing ratios. *Proc. Struct. Integr.* 37:383–388, 2022.
- Goyal, A., et al. In situ synthesis of metal nanoparticle embedded free standing multifunctional PDMS films. *Macromol. Rapid Commun.* 30:1116, 2009.
- Johnston, I. D., D. K. McCluskey, C. K. L. Tan, and M. C. Tracey. Mechanical characterization of bulk Sylgard 184 for microfluidics and microengineering. *J. Micromech. Microeng.* 24:035017, 2014.



- Ramo, N. L., K. L. Troyer, and C. M. Puttlitz. Viscoelasticity of spinal cord and meningeal tissues. *Acta. Biomaterilia*. 75:253– 262, 2018.
- 42. Campeau, M.-A., et al. Effect of manufacturing and experimental conditions on the mechanical and surface properties of silicone elastomer scaffolds used in endothelial mechanobiological studies. *Biomed. Eng. Online.* 16:90, 2017.
- Chen, A. I., et al. Multilayered tissue mimicking skin and vessel phantoms with tunable mechanical, optical, and acoustic properties. *Int. J. Med. Phys. Res. Pract.* 43:3117, 2016.
- 44. Lakes, R. "Viscoelastic properties of materials," *Viscoelast. Mater.*, 2010.
- Zacharatos, A., and E. Kontou. Nonlinear viscoelastic modeling of soft polymers. J. Appl. Polym. Sci. 2015. https://doi.org/10.1002/ app.42141.
- Hadley, D. W., and I. M. Ward. Anisotropic and nonlinear viscoelastic behaviour in solid polymers. *Rep. Prog. Phys.* 38(10):1143– 1215, 1975.

Fehervary, H., M. Smoljkic, J. Vander Sloten, and N. Famaey. Planar biaxial testing of soft biological tissue using rakes: a critical analysis of protocol and fitting process. *J. Mech. Behav. Biomed. Mater.* 61:135–151, 2016.

Publisher's Note Springer Nature remains neutral with regard to jurisdictional claims in published maps and institutional affiliations.

Springer Nature or its licensor (e.g. a society or other partner) holds exclusive rights to this article under a publishing agreement with the author(s) or other rightsholder(s); author self-archiving of the accepted manuscript version of this article is solely governed by the terms of such publishing agreement and applicable law.

